THE JOURNAL OF PHYSICAL CHEMISTRY Letters

Cite This: J. Phys. Chem. Lett. 2018, 9, 4087−4095

Letter

pubs.acs.org/JPCL

Triplet Energy Transfer Governs the Dissociation of the Correlated Triplet Pair in Exothermic Singlet Fission

Tia S. Lee,[†] YunHui L. Lin,[‡] Hwon Kim,[†] Ryan D. Pensack,[†,#] Barry P. Rand,[‡,§] and Gregory D. Scholes*[,†]

[†]Department of Chemistry, Princeton University, Princeton, New Jersey 08544, United States

[‡]Department of Electrical Engineering, Princeton University, Princeton, New Jersey 08544, United States

[§]Andlinger Center for Energy and the Environment, Princeton University, Princeton, New Jersey 08544, United States

Supporting Information

ABSTRACT: Singlet fission is a spin-allowed process of exciton multiplication that has the potential to enhance the efficiency of photovoltaic devices. The majority of studies to date have emphasized understanding the first step of singlet fission, where the correlated triplet pair is produced. Here, we examine separation of correlated triplet pairs. We conducted temperature-dependent transient absorption on 6,3-bis(tri*iso*propylsilylethynyl)pentacene (TIPS-Pn) films, where singlet fission is exothermic. We evaluated time constants to show that their temperature dependence is inconsistent with an exclusively thermally activated process. Instead, we found that the trends can be modeled by a triplet−triplet energy transfer. The fitted reorganization energy and electronic coupling agree closely with values calculated using density matrix renormalization group quantum-chemical theory. We conclude that dissociation of the correlated triplet pair to separated (but spin-entangled) triplet excitons in TIPS-Pn occurs by triplet−triplet energy transfer with a hopping time constant of approximately 3.5 ps at room temperature.

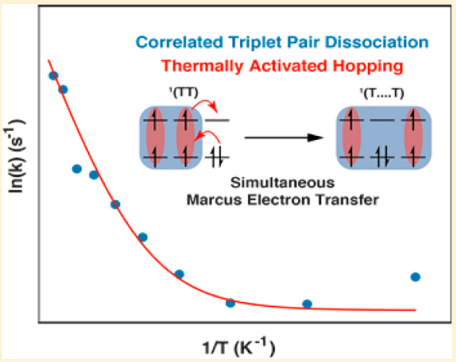

Singlet fission converts a singlet exciton (S_1)—in many cases, effectively localized on one molecule—into a correlated triplet-pair (CTP) state, ^{1}(TT), shared over two neighboring molecules. The CTP state is a doubly excited "dark" intermediate state with overall singlet character.[1−3] Among the chemical systems exhibiting singlet fission, two extensively investigated systems are tetracene[4−6] and pentacene.[1,3,7,8] Owing to their favorable energetics and electronic couplings relevant to singlet fission, these systems exhibit quantitative triplet yields approaching 200%. Harvesting two triplet excitons relies not only on the intrinsic yield of CTPs but also on the efficacy of successive events. For example, the formation of separated triplet excitons requires dephasing of the spin-entangled CTP state. To elucidate this dephasing, we need to better understand the evolution of ^{1}(TT). How is triplet character manifested following the formation of the CTP state? The state should eventually lose spin correlation and become two independent triplet excitons ($T_1 + T_1$) localized on individual chromophores. Prior to that, the triplet excitations may experience spatial separation while nonetheless retaining their spin correlation.[9,10] Here, we investigate the mechanism by which the CTP evolves into separated triplet excitons.

Previous work has suggested that the nascent CTP does dissociate, leading to the following kinetic scheme.[11]

$$S_0 + S_1 \rightarrow {}^1(\mathrm{TT}) \rightarrow {}^1(\mathrm{T}\cdots\mathrm{T}) \rightarrow T_1 + T_1 \quad (1)$$

This model includes two CTP intermediates, ^{1}(TT) and ^{1}(T···T). The nascent, initial CTP is denoted by ^{1}(TT), whereas ^{1}(T···T) represents the subsequent separated (but still spin-correlated) triplet pair. Considering that singlet fission generates triplets with strikingly high quantum yield, it has been surmised that the fusion of triplet pairs [^{1}(TT) → S_0 + S_1] is thermodynamically disfavored compared to their dissociation, [^{1}(TT) → ^{1}(T···T)]. The exact mechanism by which CTP undergoes dissociation still remains unclear. One hypothesis is that the CTP is a bound excimer with finite binding energy—likening its spatial separation to excimer dissociation.[12] Alternatively, triplet−triplet energy transfer has been invoked to account for spatial dissociation of ^{1}(TT).[9−11] Theoretical formulations predict retention of the spin component of the wave function even following triplet energy transfer.[10] Although much progress has been made to understand the spectroscopic properties of the CTP,[11] many questions still remain regarding its evolution to the $T_1 + T_1$ state.

Transient absorption (TA) spectroscopy has placed substantial emphasis on understanding the formation of the CTP. However, considerably fewer studies have investigated later steps of the process. Herein, we employ TA to detect and

Received: June 12, 2018
Accepted: July 5, 2018
Published: July 5, 2018

DOI: 10.1021/acs.jpclett.8b01834
J. Phys. Chem. Lett. 2018, 9, 4087−4095

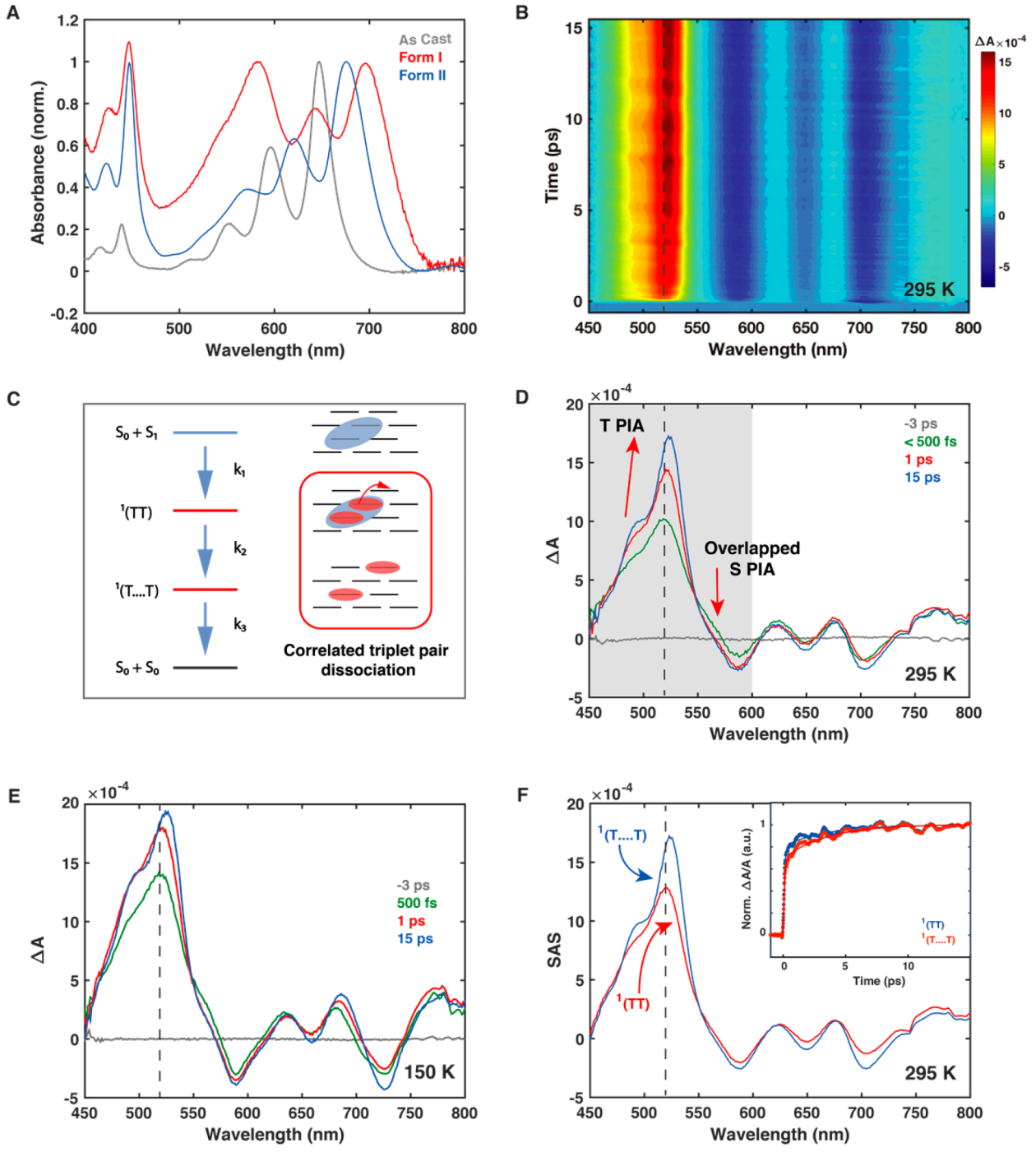

Figure 1. Summary of TA of the 2D-brickwork TIPS-Pn film at 298 K. (A) Room-temperature absorption spectra of as-cast (gray), Form I (red), and Form II (blue) TIPS-Pn films. (B) Contour map of 2D-brickwork TIPS-Pn film TA at 295 K. (C) Schematic representation of a three-component kinetic scheme applied to global analysis. TA spectra of 295 (D) and 150 K (E) at selected delay times of −3 ps (gray), <500 fs (green), 1 ps (red), and 15 ps (blue). (F) 295 K species associated spectra (SAS) of ^{1}(TT) and ^{1}(T···T) in red and blue, respectively, obtained from global analysis. The inset displays kinetics extracted at 518 (blue) and 525 nm (red), corresponding to maxima of ^{1}(TT) and ^{1}(T···T), respectively. Dashed lines in this figure were added as a guide to the eye.

distinguish between the ^{1}(TT) and ^{1}(T···T) intermediate species. We provide compelling evidence that CTP dissociation is governed by triplet−triplet energy transfer.

We study 6,3-bis(tri*iso*propylsilylethynyl)pentacene (TIPS-Pn)—a system in which singlet fission is exergonic with nearly 200% yield.[13−15] Polycrystalline films of TIPS-Pn, adopting Form I 2D-brickwork and Form II brickwork motifs, are prepared via solvent and thermal annealing, respectively, as reported by Grieco *et al.*[16] Steady-state absorption spectra at 298 K of Form I and II TIPS-Pn (Figure 1A) show characteristic vibronic progressions in the S_1 manifold, in agreement with previously reported spectra.[16,17] The spectra recorded as a function of temperature (Supporting Information Figure S2) show a red shift in peak position as the temperature is lowered, which results from changes in lattice−phonon interactions.[18−20] The TA contour map for the Form I TIPS-

DOI: 10.1021/acs.jpclett.8b01834
J. Phys. Chem. Lett. 2018, 9, 4087−4095

Pn film at 295 K is shown in Figure 1B. Spectra at selected delay times are displayed in Figure 1D. Negative features in the 550−750 nm range, characteristic of ground-state bleach (GSB), reflect distinctive absorption line shapes. Positive features at 450−575 nm are characteristic of photoinduced absorption (PIA). At 1 and 15 ps, TA spectra display triplet PIA (T PIA), $T_1 \rightarrow T_n$, spanning from 450 to 550 nm. The TA spectrum prior to 500 fs exhibits an additional positive feature to the red side of 550 nm, arising from the convoluted broad singlet PIA (S PIA), $S_1 \rightarrow S_n$, which spans 450−575 nm. That S PIA transitions into T PIA within a few hundred femtoseconds is indicative of singlet fission. These features are in good agreement with previously reported room-temperature TA of TIPS-Pn films.[15,16,21,22]

Examination of the spectral evolution in Figure 1D reveals dynamics of the CTP. For instance, the maximum of the T PIA feature exhibits a slight spectral shift from ca. 518 nm toward red wavelengths, accompanied by increased intensity. Overlapping features in the 450−575 nm spectral window complicate extraction of the dynamics arising solely from this feature, but the kinetics are resolved more clearly by exploiting global analysis. Global analysis is often used in systems with overlapping spectroscopic features, allowing extraction of the distinct components contributing to the dynamics.[23,24] We applied global analysis with both two- and three-component kinetic schemes and found that the three-component scheme represents the best fit to the experimental data. Therefore, the mechanism for singlet fission in the TIPS-Pn system involves two distinct intermediate CTPs, ^{1}(TT) and ^{1}(T···T).

Global analysis serves to distinguish the electronically and spin-coupled CTP from the electronically decoupled CTP. A schematic representation of the three-component kinetic model is presented in Figure 1C, where k_1 describes the initial photogenerated singlet exciton forming a *nascent* CTP intermediate ^{1}(TT). Then, ^{1}(TT) dissociates to form the *spatially separated* CTP intermediate ^{1}(T···T), corresponding to k_2. Subsequent evolution of ^{1}(T···T), including spin decoherence of the triplet pair and decay to the ground state, is represented by k_3. The ^{1}(T···T) state is defined as a triplet pair that is electronically decoupled while remaining spin-entangled. Moving to the three-component model allows for both triplet-pair states to be unveiled. Previously, this three-component kinetic model has been applied to describe singlet-fission dynamics involving two triplet-pair states.[11,15,25,26] The number of distinguishable components contributing to the dynamics was determined on the basis of root-mean-squared values and residuals.[24,27] Details of the analysis are discussed in the Supporting Information. The two-component model was shown to inadequately model the data, while the three-component scheme resulted in significant improvement of the fit.

Species associated spectra (SAS), displayed in Figure 1F, were simulated via global analysis for the second and third components. For the third component, SAS indeed exhibits a slight red shift compared to the second component. Overall, SAS of the second and third components are consistent with TA spectra at 1 and 15 ps, respectively, shown in Figure 1D. Similar observations of red-shifted T PIA have been reported for pentacene and tetracene derivatives and have been assigned to ^{1}(T···T).[11,12,25] Hence, we assign the red-shifted PIA feature as ^{1}(T···T). As mentioned in the introduction, theoretical and experimental justification exists for the triplet pair undergoing spatial separation (while maintaining spin correlation) prior to forming independent triplets.[10−12,28] The inset of Figure 1F displays single-wavelength kinetics extracted at 518 and 525 nm, which correspond to the maxima of ^{1}(TT) and ^{1}(T···T), respectively. Notably, consistent with the proposed three-component scheme, ^{1}(T···T) exhibits a delayed rise relative to ^{1}(TT).

Triplet-pair separation by excimer dissociation and triplet energy transfer are both thermally activated processes. To quantify thermal activation of CTP separation, temperature-dependent measurements were conducted. Previously, Stern *et al.*[29] reported the temperature dependence of the dynamics of intermediate triplet pairs in endothermic singlet fission. Yong *et al.*[30] demonstrated that the CTP state in endothermic singlet fission is stabilized compared to two independent triplets, and the observed temperature dependence of triplet-pair separation is governed largely by the barrier arising from this stabilization energy. In TIPS-Pn, where singlet fission is exothermic, the CTP state experiences no such stabilization. Hence, the observed temperature dependence is a direct reflection of triplet separation. The ^{1}(T···T) state is a relatively new concept, and experimental studies invoking the ^{1}(T···T) state have focused on distinguishing between the spectral features of ^{1}(T···T) and ^{1}(TT)[11,15] while their temperature-dependent behaviors have remained underexplored.[25,26,31,32] In our study, we expand our understanding of the intermediate triplet pair by combining spectral delineation of the ^{1}(TT) and ^{1}(T···T) states with temperature-dependent measurements.

In the low-temperature range surveyed in this work, the Form I TIPS-Pn film displays similar TA spectral features (GSB, S PIA, and T PIA) as those in the 298 K spectrum. Qualitatively, a similar red-shifted T PIA assigned to ^{1}(T···T) is observed over the temperatures surveyed. The extent of such an effect, however, becomes less prominent as the temperature is lowered to 77 K. Moreover, slower spectral conversion is apparent at these lower temperatures. Comparison of 1 and 15 ps spectra, representing ^{1}(TT) and ^{1}(T···T), respectively, for 295 and 150 K in Figure 1D,E reveals such a difference in rate and magnitude of red-shifted T PIA behavior.

Rate parameters extracted from the three-component model are summarized in Table 1. In exothermic singlet fission, separation of the CTP (k_2) is expected to be reversible. However, our effort to evaluate the equilibrium model resulted in a poor fit, as assessed by residuals. Examination of temperature-dependent rate parameters reveals that k_1 is temperature-independent, confirming that singlet fission is not a thermally activated process. This observation is strikingly

Table 1. Summary of Form I TIPS-Pn Rate Parameters Obtained from Global Analysis at Various Temperatures

temperature (K)	k_1 (ps^{-1}); τ_1 (fs)	k_2 (ps^{-1}); τ_2 (ps)	k_3 (ps^{-1}); τ_3 (ps)
78	10.7; 93.1	0.063; 15.9	1.15×10^{-3}; 872
100	10.0; 100	0.057; 17.6	7.34×10^{-4}; 1360
125	10.3; 97.1	0.052; 19.4	1.31×10^{-3}; 762
150	9.93; 101	0.064; 15.6	1.47×10^{-3}; 679
175	10.8; 92.7	0.085; 11.8	1.41×10^{-3}; 707
200	10.4; 96.6	0.108; 9.23	1.43×10^{-3}; 700.
225	10.2; 97.8	0.135; 7.39	1.44×10^{-3}; 694
250	8.98; 111	0.142; 7.06	2.61×10^{-4}; 3830
275	10.9; 92.0	0.257; 3.89	4.67×10^{-4}; 2140
295	12.1; 82.9	0.286; 3.50	8.87×10^{-5}; 11300

DOI: 10.1021/acs.jpclett.8b01834
J. Phys. Chem. Lett. 2018, 9, 4087−4095

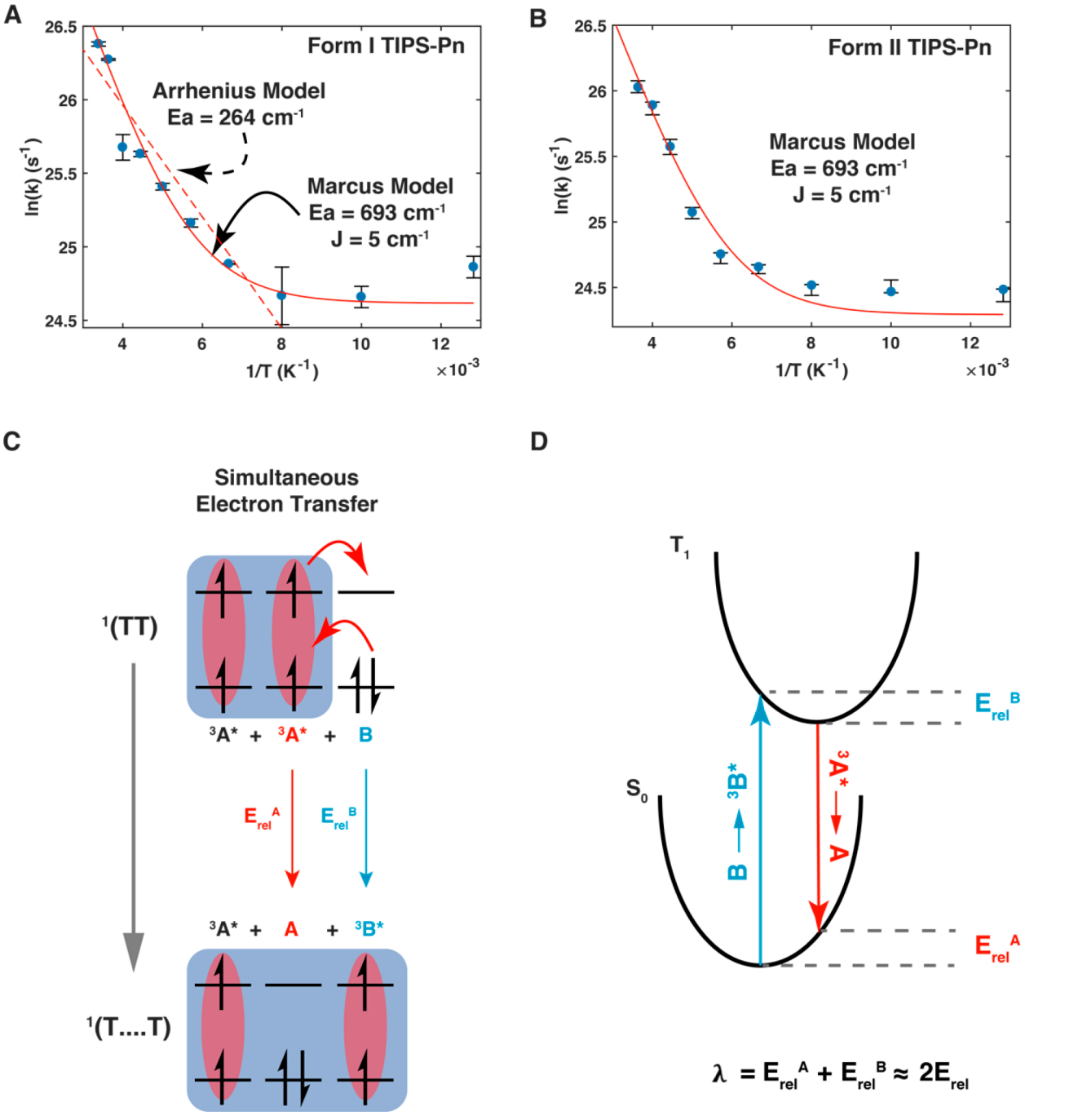

Figure 2. Correlated triplet-pair separation. Rate parameter for separation (blue dots) of the correlated triplet pair, ^{1}(TT) → ^{1}(T···T), against the inverse temperature $(1/T)$. (A) Form I TIPS-Pn film where the red dashed line represents the fit of the higher-temperature regime with the Arrhenius model. The solid red line represents the Marcus model fit. (B) Form II TIPS-Pn film modeled with Marcus treatment for triplet−triplet energy transfer with the same microscopic parameters as the Form I TIPS-Pn film. (C) Schematic illustration of triplet energy transfer in Marcus description implemented for separation of the correlated triplet pair in singlet fission. (D) Process of donor relaxation and acceptor excitation, A and B, respectively. The associated geometry relaxation energies E_{rel}^{A}, and (E_{rel}^{B}) are indicated.

different from thermally activated triplet-pair formation reported in single crystals of tetracene, where singlet fission is endoergic.[33] Unlike the first step, k_2 of the analysis, which is attributed to spatial separation of the CTP, shows a strong temperature dependence. Subsequent processes following ^{1}(T···T), represented by k_3, would not influence the interpretation of k_2, considering that their rates are orders of magnitude larger than the rate-determining step. Triplet fusion (k_{-3}) is expected to be three-fold slower than k_3 due to spin restrictions on triplet−triplet annihilation.[10] This is outside of our instrument time window. Hence, k_{-3} was not included in the model.

We model the temperature dependence of k_2 with both a thermally activated Arrhenius model and a triplet−triplet energy transfer model based on two correlated electron transfers (*vide infra*). Blue dots in Figure 2A show the rate of spatial separation of the CTP (k_2), ^{1}(TT) → ^{1}(T···T), plotted against the inverse temperature $(1/T)$. In the high-

DOI: 10.1021/acs.jpclett.8b01834
J. Phys. Chem. Lett. 2018, 9, 4087−4095

temperature regime, i.e., 298−125 K, a near-linear relationship is evident. At lower temperatures, however, the value of k_2 plateaus. We first model the higher-temperature regime with an Arrhenius model (Figure 2A, dashed line)

$$k = a \exp\left(-\frac{E_a}{k_b T}\right) + b \tag{2}$$

where k_b is the Boltzmann constant, T is temperature, and E_a corresponds to the activation energy of the thermally activated process. From this model, E_a is determined to be 264 cm^{-1}. On the other hand, the model for triplet-pair separation through excimer dissociation predicts a binding energy of more than 2420 cm^{-1}.[12]

The poor fit of the Arrhenius model and the large discrepancy with the excimer dissociation model suggest that another mechanism, such as triplet−triplet energy transfer, might explain triplet-pair separation during the singlet fission process. Previous work has shown that dissociation of the triplet pair—without changing the overall spin state—can occur by triplet−triplet energy transfer. This phenomenon manifests as spatial shifts of the photoexcitations from one local site to another.[10] This is a rigorous result when assuming that the triplet pair is relatively weakly bound.

Triplet migration occurs via the so-called Dexter mechanism. For molecules, the dominant term in the electronic coupling is a virtual, simultaneous exchange of two electrons between donor and acceptor molecules.[34−36] It has been established by studying energy transfer in conjugated polymer films that the triplet energy transfer in disordered organic semiconductors can be modeled quantitatively using the framework of Marcus theory.[37−40] Figure 2C illustrates this coupled electron transfer model in the context of CTP separation. After singlet fission, the ^{1}(TT) state extends over two chromophores—each in a triplet excited state (^{3}A* + ^{3}A*) with neighboring acceptors in the ground state (B). A donor chromophore (red ^{3}A*) transfers its triplet excitation to an acceptor chromophore (B), while the other excitation in the pair (black ^{3}A*) remains localized. The overall spin character of the species is maintained in the process, thus forming the spin-correlated yet spatially decoupled ^{1}(T···T) state. That is, ^{3}A* + ^{3}A* + B → ^{3}A* + A + ^{3}B*. The reorganization energy (λ) for triplet transfer, illustrated in Figure 2D, is a sum of the geometric relaxation energies involved in the de-excitation of A (E_{rel}^{A}) and the excitation of B (E_{rel}^{B})

$$\lambda = E_{rel}^{A}(^3\text{A}^* \rightarrow \text{A}) + E_{rel}^{B}(\text{B} \rightarrow {}^3\text{B}^*) \approx 2E_{rel} \tag{3}$$

Within the Marcus framework applied to triplet−triplet energy transfer, the rate of transfer is governed by eq 4

$$\text{Rate} = \frac{2\pi}{\hbar} J^2 \sqrt{\frac{1}{4\pi k_b \lambda T}} \exp\left(-\frac{E_a}{k_b T}\right) \tag{4}$$

where J is the triplet transfer integral, E_a is the activation energy involved in the triplet transfer, k_b is the Boltzmann constant, and T is temperature. E_a is described by eq 5

$$E_a = \frac{\lambda}{4}\left(1 + \frac{\Delta G^0}{\lambda}\right) \approx \frac{E_{rel}}{2} \tag{5}$$

where ΔG^0 is the Gibbs free-energy difference between the donor and acceptor. In the case of triplet transfer between two identical TIPS-Pn molecules, ΔG^0 is zero and E_a is only a function of the reorganization energy, λ.

These parameters can be extracted from the temperature-dependent reaction rates shown in Figure 2A for Form I TIPS-Pn. The solid red line in Figure 2A shows the fit of the triplet transfer model to k_2 as a function of T. We thus obtain an activation energy of 693 cm^{-1}, and because $E_a = \lambda/4$, this implies a reorganization energy of 2770 cm^{-1}, and we find a triplet transfer integral of ca. 5 cm^{-1}. To further test the reliability of the proposed model, we performed a replica temperature-dependent TA experiment on Form II TIPS-Pn and applied a three-component kinetic scheme global analysis. From these data, k_2 is plotted against $1/T$, as shown by blue dots in Figure 2B. The solid red curve in Figure 2B represents the fit based on eq 4, demonstrating that the same set of microscopic parameters E_a and λ are applicable in Form II TIPS-Pn. Previously, a similar expression based on the Marcus−Levich−Jortner rate model was used by Yong *et al.*[30] to model the temperature dependence of CTP dynamics.

As self-exchange reorganization energy for single electron transfer in pentacene derivatives is predicted to be approximately 1400 cm^{-1},[41] it is understandable that the result that we derived for a two-electron transfer in TIPS-Pn (λ = 2770 cm^{-1}) is approximately twice that of the predicted single-electron transfer. A triplet transfer integral of 0.14 cm^{-1} has been reported for disordered platinum−polymer thin films.[37−39] Density functional theory (DFT) predicts that for acenes the triplet transfer integral is in the range of 0.01−10 cm^{-1}.[28,42,43] Because in these systems the triplet ground state can be adequately described by a single configuration, DFT is an accurate method for calculating electronic structure. On the basis of these comparisons, both the reorganization energy and triplet transfer integral derived from our model are consistent with prior theoretical predictions.

To further support our analysis, we calculated λ and J in a dimer system using the methods described below. Resolving the electronic structure associated with the acene family of molecules requires quantum-chemical methodologies that explicitly compute the full physical character of correlated wave functions, as shown in the manifestation of radical character in singlet ground states.[44] The multireference techniques involving complete active space (CAS) computation have been used successfully to predict excitation energies in acenes[45] and were recently implemented in several studies to investigate electronic states involved in singlet fission.[2,46,47] The clear downside of the multireference methods is the exponential scaling of computational cost upon increasing the active space of correlated electrons and orbitals. The density matrix renormalization group (DMRG) algorithm[48−50] provides a means of bypassing the exponential scaling of computational cost and allows expansion of the active space beyond the traditional CAS method limit of 16 orbitals to treat the static (valence-electron) correlation energy, finding use in systems ranging from small molecules[51] at the nascent stage of the algorithm to complex molecules such as transition metal complexes.[52]

Using DMRG methods, we calculate λ and J values of 2660 and 30.6 cm^{-1}, respectively. The computed λ is obtained by halving the energy gap of the two states of interest, which are the states before and after the triplet energy transfer. While J also contributes to the energy gap, its expected value on the order of 10 cm^{-1} is negligible compared to λ. Therefore, the total energy difference is a reasonable estimate of λ. However, calculations typically overestimate J due to inherent limitations of strong coupling in the Born−Oppenheimer approximation,

DOI: 10.1021/acs.jpclett.8b01834
J. Phys. Chem. Lett. 2018, 9, 4087−4095

which does not take vibronic quenching into consideration, as demonstrated by Ottiger.[53] Therefore, our experimentally derived triplet transfer reorganization energy (λ = 2770 cm^{-1}) is in strikingly good agreement with our computational prediction (λ = 2660 cm^{-1}). Taken together, these results provide strong evidence that triplet-pair dissociation in TIPS-Pn films is governed by a triplet−triplet energy transfer process.

The temperature dependence of k_2 exhibits exponential, thermally activated behavior at ambient temperatures but becomes temperature-independent at lower temperatures (125−78 K). That trend is also captured by our model. This trend can be explained by the way spectral line broadening contributes to the spectral overlap for energy transfer.[54] The temperature-dependent regime is found when the homogeneous line broadening is larger than inhomogeneous line broadening. At lower temperatures, the disorder of the polycrystalline material dominates over the homogeneous line broadening and the spectral line broadening, and the spectral overlap that ensures energy conservation for energy transfer becomes temperature-independent.

In summary, we have investigated the mechanism and temperature dependence of singlet fission dynamics in polycrystalline Form 1 and Form II TIPS-Pn. Global analysis with a three-component kinetic model [$S_0 + S_1 \rightarrow {}^1(TT) \rightarrow {}^1(T\cdots T) \rightarrow T_1 + T_1$] permitted us to differentiate contributions from $^1(T\cdots T)$ and $^1(TT)$ in a congested spectral region. Moreover, global analysis was applied to fit TA dynamics over a wide temperature range. Like the previously reported excimer-dissociation model, the triplet energy transfer model reported in this work exhibits strong correlation with temperature. We quantified this correlation by comparing the experimental data to both a simple Arrhenius model and a more sophisticated model based on triplet energy transfer. Ultimately, the triplet transfer model offers the best explanation of triplet-pair dissociation in the TIPS-Pn system. Using the Marcus thermally activated hopping model of triplet transfer, we were able to extract the activation barrier (reorganization energy) and the triplet transfer integral associated with triplet-pair dissociation. Our experimental reorganization energy is in excellent agreement with quantum chemical calculations using the DMRG method. A recent report[30] interpreted activated energy transfer to indicate stabilization of the parent CTP in endothermic singlet fission. By contrast, in exothermic singlet fission, our analysis of the activation in conjunction with fitting of the temperature-independent regime—supported by quantum-chemical calculation—suggests that triplet-pair separation and the effective barrier for that separation can be understood through the physics of triplet energy transfer.

METHODS

Thin-Film Preparation. HPLC-grade (99%) TIPS-Pn was purchased from Sigma-Aldrich and used as received. TIPS-Pn was dissolved in chloroform at a concentration of 10 mg/mL. Sapphire substrates were cleaned by sequential sonication in deionized water, acetone, and isopropanol prior to treatment by O_2 plasma. The TIPS-Pn solution then was spin-coated on substrates at 2000 rpm for 60 s in ambient air. Subsequently, films were exposed to toluene vapor for 5 min for the Form I TIPS-Pn film, while Form II TIPS-Pn films were placed on a hot plate in ambient air at 130 °C for 10 min.

Temperature-Dependent Spectroscopy. Steady-state absorption measurements were carried out using an Agilent Cary 6000i UV−vis−NIR spectrophotometer (Agilent Technologies, Santa Clara, California). Typical parameters for collection of absorption spectra are a step size of 1 nm, band-pass of 2 nm, and integration period of 0.2 s.

Ultrafast TA measurements were conducted with a 1 kHz Ti:sapphire regenerative amplifier system (Coherent Libra, Santa Clara, California). Libra outputs ∼800 nm pulses with ∼45 fs temporal resolution with approximately 4 W power. Output of the laser amplifier is separated with a beamsplitter and further used in pump and probe beams. The pump part of the Libra output was directed to an optical parametric amplifier (Light Conversion OPerA, Vilnius, Lithuania), which then converted the 800 nm Libra output into 700 and 675 nm for Forms I and II, respectively, to ensure resonant excitation of the sample. The probe part of the Libra output was directed to a commercial TA spectrometer (Ultrafast System Helios, Sarasota, Florida) and used in generation of a visible light continuum, in the ∼400−800 nm spectral region. Optical filters were incorporated in order to separate out the 800 nm radiation. TA measurements were performed at magic angle conditions. Polarization of the pump relative to the probe was controlled with a combination of a $\lambda/2$ waveplate and polarizer in both the pump (situated just before the sample) and probe (situated before continuum generation) beam paths. The optical density of the Form I and II samples ranged from ca. 0.07 to 0.16 at the excitation wavelength.

The pump beam spot size was estimated by analyzing the image obtained by a digital CCD camera (Thorlabs Inc., Newton, New Jersey) with Thorcam Software (Thorlabs Inc., Newton, New Jersey). The camera was placed at the pump probe overlap. The pump beam size of the wavelength at ca. 700 nm was approximately 150 μm. The pump power was measured with a high-sensitivity optical power sensor (Coherent, Santa Clara, California). Incident pump power in the visible was ∼10 μW, and the probe power was below 2.5 μW. Each measurement was averaged with ∼100 scans to achieve high signal-to-noise ratios necessary for global analysis.

Steady-state absorption and TA in cryogenic conditions were performed in vacuum using a Janis ST-100 liquid nitrogen optical cryostat (Janis Research, Woburn, Massachusetts). For steady-state absorption measurements, the cryostat was coupled with a vacuum pump (GE Motors, Boston, Massachusetts) in conjunction with a Turbotronik NT 10 turbo pump (Leybold Vacuum, Cologne, Germany). The pressure was monitored via a TPG 361 controller for single gauge (Pfeiffer Vacuum GmbH, Nashua, New Hampshire). The typical pressure for the temperature-dependent absorption was approximately 5.0 × 10^{-6} mbar. For ultrafast TA measurement, a HiCube 80 Eco (Pfeiffer Vacuum GmbH, Nashua, New Hampshire) was used to achieve vacuum and to monitor the pressure. The typical pressure for the temperature-dependent TA was approximately 1.0 × 10^{-6} mbar. Temperature variability was achieved by a Lakeshore 311 temperature controller (LakeShore Cryotronics, Westerville, Ohio) for both steady-state absorption and TA experiments.

Calculations of the Reorganization Energy and Triplet Transfer Integral. Calculations of the reorganization energy (λ) and triplet transfer integral (J) of TIPS-Pn were performed on a dimer of trimethylsilylethynyl (TMS)-pentacene, which was adopted in lieu of TIPS-Pn to reduce computational cost. The orientation of the two monomers was set according to the

DOI: 10.1021/acs.jpclett.8b01834
J. Phys. Chem. Lett. 2018, 9, 4087−4095

crystal structure.[55] In the reorganization energy calculation, one monomer was optimized to the singlet ground-state geometry and the other to the first exited triplet state. In triplet transfer integral calculations, both of the monomers were optimized to the triplet geometry. Both the reorganization energy and triplet transfer integral were computed from the energy gap of the triplet ground state and the first excited triplet state of the dimer system in their respective geometries.

Geometry optimization was performed using Gaussian 16 on DFT with the B3LYP functional[56] level of theory with the 6-31G* basis set. In addition, the LANL2DZ basis set[57] on silicon and the d-polarization function[58] were applied to describe inner electrons with effective core potentials and outer electrons with a double-ζ basis.

The reorganization energy was computed using PySCF[59] interfaced with BLOCK[60] DMRG using the state-averaged density matrix renormalization group self-consistent field (SA-DMRGSCF) method.[61] Twenty-four molecular orbitals obtained from restricted Hartree−Fock (RHF) theory were included in the active space comprised of 12 occupied orbitals and 12 unoccupied orbitals. The selection therefore gives 24 electrons in 24 orbitals for the active space. The ground triplet state and first excited triplet state were averaged with 0.5 weight each on the SA-DMRGSCF step. The DMRG algorithm was adapted to alleviate the computational cost of the large active space used. Dunning's double-ζ basis set was used for every atom.[62,63] The active space used in the calculation consisted exclusively of π-orbitals, with the 12 highest filled π-type orbitals and the 12 lowest unoccupied π-type orbitals from the initial RHF calculation. A bond dimension of M = 1000 was used.

■ ASSOCIATED CONTENT

Supporting Information

The Supporting Information is available free of charge on the ACS Publications website at DOI: 10.1021/acs.jpclett.8b01834.

Absorption spectra of TIPS-Pn in various material platforms, temperature-dependent spectroscopy data, additional experimental details for ultrafast transient absorption experiments, power-dependent transient absorption data, selected temperature-dependent transient absorption data, additional details and discussion on global analysis, and details of the computational method and result. (PDF)

■ AUTHOR INFORMATION

Corresponding Author

*E-mail: gscholes@princeton.edu.

ORCID

Tia S. Lee: 0000-0003-0635-6668
YunHui L. Lin: 0000-0002-0817-8757
Barry P. Rand: 0000-0003-4409-8751
Gregory D. Scholes: 0000-0003-3336-7960

Present Address

#R.D.P.: Micron School of Materials Science & Engineering, Boise State University, Boise, Idaho 83725, U.S.A.

Notes

The authors declare no competing financial interest.

■ ACKNOWLEDGMENTS

G.D.S. acknowledges support from the Division of Chemical Sciences, Geosciences, and Biosciences, Office of Basic Energy Sciences of the U.S. Department of Energy through Grant No. DE-SC0015429. We acknowledge support from a Taylor Fellowship, Princeton University. B.P.R. and Y.L.L. thank the National Science Foundation Award No. CBET-1604524. The authors thank D. Oblinsky for designing the cryostat.

■ REFERENCES

(1) Jundt, C.; Klein, G.; Sipp, B.; Lemoigne, J.; Joucla, M.; Villaeys, A. A. Exciton Dynamics in Pentacene Thin-Films Studied by Pump-Probe Spectroscopy. *Chem. Phys. Lett.* **1995**, *241* (1−2), 84−88.

(2) Zimmerman, P. M.; Zhang, Z. Y.; Musgrave, C. B. Singlet Fission in Pentacene Through Multi-Exciton Quantum States. *Nat. Chem.* **2010**, *2* (8), 648−652.

(3) Wilson, M. W. B.; Rao, A.; Clark, J.; Kumar, R. S. S.; Brida, D.; Cerullo, G.; Friend, R. H. Ultrafast Dynamics of Exciton Fission in Polycrystalline Pentacene. *J. Am. Chem. Soc.* **2011**, *133* (31), 11830−11833.

(4) Merrifiels, R. E.; Avakian, P.; Groff, R. P. Fission of Singlet Excitons into Pairs of Triplet Excitons in Tetracene Crystals. *Chem. Phys. Lett.* **1969**, *3* (9), 728−7280.

(5) Burdett, J. J.; Bardeen, C. J. Quantum Beats in Crystalline Tetracene Delayed Fluorescence Due to Triplet Pair Coherences Produced by Direct Singlet Fission. *J. Am. Chem. Soc.* **2012**, *134* (20), 8597−8607.

(6) Burdett, J. J.; Bardeen, C. J. The Dynamics of Singlet Fission in Crystalline Tetracene and Covalent Analogs. *Acc. Chem. Res.* **2013**, *46* (6), 1312−1320.

(7) Smith, M. B.; Michl, J. Singlet Fission. *Chem. Rev.* **2010**, *110* (11), 6891−6936.

(8) Smith, M. B.; Michl, J. Recent Advances in Singlet Fission. *Annu. Rev. Phys. Chem.* **2013**, *64*, 361−386.

(9) Srimath Kandada, A. R.; Petrozza, A.; Lanzani, G. Ultrafast Dissociation of Triplets in Pentacene Induced by an Electric Field. *Phys. Rev. B: Condens. Matter Mater. Phys.* **2014**, *90* (7), 075310.

(10) Scholes, G. D. Correlated Pair States Formed by Singlet Fission and Exciton-Exciton Annihilation. *J. Phys. Chem. A* **2015**, *119* (51), 12699−12705.

(11) Pensack, R. D.; Ostroumov, E. E.; Tilley, A. J.; Mazza, S.; Grieco, C.; Thorley, K. J.; Asbury, J. B.; Seferos, D. S.; Anthony, J. E.; Scholes, G. D. Observation of Two Triplet-Pair Intermediates in Singlet Exciton Fission. *J. Phys. Chem. Lett.* **2016**, *7* (13), 2370−2375.

(12) Stern, H. L.; Musser, A. J.; Gelinas, S.; Parkinson, P.; Herz, L. M.; Bruzek, M. J.; Anthony, J.; Friend, R. H.; Walker, B. J. Identification of a Triplet Pair Intermediate in Singlet Exciton Fission in Solution. *Proc. Natl. Acad. Sci. U. S. A.* **2015**, *112* (25), 7656−7661.

(13) Anthony, J. E.; Eaton, D. L.; Parkin, S. R. A Road Map to Stable, Soluble, Easily Crystallized Pentacene Derivatives. *Org. Lett.* **2002**, *4* (1), 15−18.

(14) Pensack, R. D.; Tilley, A. J.; Parkin, S. R.; Lee, T. S.; Payne, M. M.; Gao, D.; Jahnke, A. A.; Oblinsky, D. G.; Li, P. F.; Anthony, J. E.; Seferos, D. S.; Scholes, G. D. Exciton Delocalization Drives Rapid Singlet Fission in Nanoparticles of Acene Derivatives. *J. Am. Chem. Soc.* **2015**, *137* (21), 6790−6803.

(15) Pensack, R. D.; Grieco, C.; Purdum, G. E.; Mazza, S. M.; Tilley, A. J.; Ostroumov, E. E.; Seferos, D. S.; Loo, Y. L.; Asbury, J. B.; Anthony, J. E.; Scholes, G. D. Solution-Processable, Crystalline Material for Quantitative Singlet Fission. *Mater. Horiz.* **2017**, *4* (5), 915−923.

(16) Grieco, C.; Doucette, G. S.; Pensack, R. D.; Payne, M. M.; Rimshaw, A.; Scholes, G. D.; Anthony, J. E.; Asbury, J. B. Dynamic Exchange During Triplet Transport in Nanocrystalline TIPS-Pentacene Films. *J. Am. Chem. Soc.* **2016**, *138* (49), 16069−16080.

(17) Diao, Y.; Lenn, K. M.; Lee, W. Y.; Blood-Forsythe, M. A.; Xu, J.; Mao, Y. S.; Kim, Y.; Reinspach, J. A.; Park, S.; Aspuru-Guzik, A.; Xue, G.; Clancy, P.; Bao, Z. N.; Mannsfeld, S. C. B. Understanding

DOI: 10.1021/acs.jpclett.8b01834
J. Phys. Chem. Lett. 2018, 9, 4087−4095

Polymorphism in Organic Semiconductor Thin Films Through Nanoconfinement. *J. Am. Chem. Soc.* **2014**, *136* (49), 17046−17057.
(18) Birks, J. B. *Organic molecular photophysics*; 1975; Vol. 2, pp 9−10.
(19) Meyer, B. *Low temperature spectroscopy*; 1971; pp 49−50.
(20) Hesse, R.; Hofberger, W.; Bassler, H. Absorption-Spectra of Disordered Solid Tetracene and Pentacene. *Chem. Phys.* **1980**, *49* (2), 201−211.
(21) Yost, S. R.; Lee, J.; Wilson, M. W. B.; Wu, T.; McMahon, D. P.; Parkhurst, R. R.; Thompson, N. J.; Congreve, D. N.; Rao, A.; Johnson, K.; Sfeir, M. Y.; Bawendi, M. G.; Swager, T. M.; Friend, R. H.; Baldo, M. A.; Van Voorhis, T. A Transferable Model for Singlet-Fission Kinetics. *Nat. Chem.* **2014**, *6* (6), 492−497.
(22) Musser, A. J.; Liebel, M.; Schnedermann, C.; Wende, T.; Kehoe, T. B.; Rao, A.; Kukura, P. Evidence for Conical Intersection Dynamics Mediating Ultrafast Singlet Exciton Fission. *Nat. Phys.* **2015**, *11* (4), 352−357.
(23) van Stokkum, I. H. M.; Larsen, D. S.; van Grondelle, R. Global and Target Analysis of Time-Resolved Spectra. *Biochim. Biophys. Acta, Bioenerg.* **2004**, *1657* (2−3), 82−104.
(24) Holzwarth, A. R. Data Analysis of Time-Resolved Spectra. In *Biophysical Techniques in Photosynthesis*; Amesz, J., Hoff, A. J., Eds.; Springer: Dordrecht, The Netherlands, 1996; pp 75−92.
(25) Breen, I.; Tempelaar, R.; Bizimana, L. A.; Kloss, B.; Reichman, D. R.; Turner, D. B. Triplet Separation Drives Singlet Fission after Femtosecond Correlated Triplet Pair Production in Rubrene. *J. Am. Chem. Soc.* **2017**, *139* (34), 11745−11751.
(26) Grieco, C.; Kennehan, E. R.; Kim, H.; Pensack, R. D.; Brigeman, A. N.; Rimshaw, A.; Payne, M. M.; Anthony, J. E.; Giebink, N. C.; Scholes, G. D.; Asbury, J. B. Direct Observation of Correlated Triplet Pair Dynamics during Singlet Fission Using Ultrafast Mid-IR Spectroscopy. *J. Phys. Chem. C* **2018**, *122* (4), 2012−2022.
(27) Alfano, R. R.; Govindjee, W. Y. R.; Becher, B.; Ebrey, T. G. Picosecond Kinetics of Fluorescence from Chromophore of Purple Membrane-Protein of Halobacterium-Halobium. *Biophys. J.* **1976**, *16* (5), 541−545.
(28) Teichen, P. E.; Eaves, J. D. Collective Aspects of Singlet Fission in Molecular Crystals. *J. Chem. Phys.* **2015**, *143* (4), 044118.
(29) Stern, H. L.; Cheminal, A.; Yost, S. R.; Broch, K.; Bayliss, S. L.; Chen, K.; Tabachnyk, M.; Thorley, K.; Greenham, N.; Hodgkiss, J.; Anthony, J.; Head-Gordon, M.; Musser, A. J.; Rao, A.; Friend, R. H. Vibronically Coherent Ultrafast Triplet-Pair Formation and Subsequent Thermally Activated Dissociation Control Efficient Endothermic Singlet Fission. *Nat. Chem.* **2017**, *9* (12), 1205−1212.
(30) Yong, C. K.; Musser, A. J.; Bayliss, S. L.; Lukman, S.; Tamura, H.; Bubnova, O.; Hallani, R. K.; Meneau, A.; Resel, R.; Maruyama, M.; Hotta, S.; Herz, L. M.; Beljonne, D.; Anthony, J. E.; Clark, J.; Sirringhaus, H. The Entangled Triplet Pair State in Acene and Heteroacene Materials. *Nat. Commun.* **2017**, *8*, 15953.
(31) Bera, K.; Douglas, C. J.; Frontiera, R. R. Femtosecond Raman Microscopy Reveals Structural Dynamics Leading to Triplet Separation in Rubrene Singlet Fission. *J. Phys. Chem. Lett.* **2017**, *8* (23), 5929−5934.
(32) Grieco, C.; Doucette, G. S.; Munro, J. M.; Kennehan, E. R.; Lee, Y.; Rimshaw, A.; Payne, M. M.; Wonderling, N.; Anthony, J. E.; Dabo, I.; Gomez, E. D.; Asbury, J. B. Triplet Transfer Mediates Triplet Pair Separation during Singlet Fission in 6,13-Bis-(triisopropylsilylethynyl)-Pentacene. *Adv. Funct. Mater.* **2017**, *27* (46), 1703929.
(33) Piland, G. B.; Bardeen, C. J. How Morphology Affects Singlet Fission in Crystalline Tetracene. *J. Phys. Chem. Lett.* **2015**, *6* (10), 1841−1846.
(34) Harcourt, R. D.; Scholes, G. D.; Ghiggino, K. P. Rate Expressions for Excitation Transfer. II. Electronic Considerations of Direct and through-Configuration Exciton Resonance Interactions. *J. Chem. Phys.* **1994**, *101* (12), 10521−10525.
(35) Scholes, G. D.; Harcourt, R. D.; Ghiggino, K. P. Rate Expressions for Excitation Transfer. III. An Ab-Initio Study of Electronic Factors in Excitation Transfer and Exciton Resonance Interactions. *J. Chem. Phys.* **1995**, *102* (24), 9574−9581.
(36) Mirkovic, T.; Ostroumov, E. E.; Anna, J. M.; van Grondelle, R.; Govindjee; Scholes, G. D. Light Absorption and Energy Transfer in the Antenna Complexes of Photosynthetic Organisms. *Chem. Rev.* **2017**, *117* (2), 249−293.
(37) Sudha Devi, L.; Al-Suti, M. K.; Dosche, C.; Khan, M. S.; Friend, R. H.; Kohler, A. Triplet Energy Transfer in Conjugated Polymers. I. Experimental Investigation of a Weakly Disordered Compound. *Phys. Rev. B: Condens. Matter Mater. Phys.* **2008**, *78* (4), 045210.
(38) Fishchuk, I. I.; Kadashchuk, A.; Sudha Devi, L.; Heremans, P.; Bassler, H.; Kohler, A. Triplet Energy Transfer in Conjugated Polymers. II. A Polaron Theory Description Addressing the Influence of Disorder. *Phys. Rev. B: Condens. Matter Mater. Phys.* **2008**, *78* (4), 045211.
(39) Hoffmann, S. T.; Scheler, E.; Koenen, J. M.; Forster, M.; Scherf, U.; Strohriegl, P.; Bassler, H.; Kohler, A. Triplet Energy Transfer in Conjugated Polymers. III. An Experimental Assessment Regarding the Influence of Disorder on Polaronic Transport. *Phys. Rev. B: Condens. Matter Mater. Phys.* **2010**, *81* (16), 165208.
(40) Kohler, A.; Bassler, H. What Controls Triplet Exciton Transfer in Organic Semiconductors? *J. Mater. Chem.* **2011**, *21* (12), 4003−4011.
(41) Gruhn, N. E.; da Silva Filho, D. A.; Bill, T. G.; Malagoli, M.; Coropceanu, V.; Kahn, A.; Bredas, J. L. The vibrational Reorganization Energy in Pentacene: Molecular Influences on Charge ransport. *J. Am. Chem. Soc.* **2002**, *124* (27), 7918−7919.
(42) Yost, S. R.; Hontz, E.; Yeganeh, S.; Van Voorhis, T. Triplet vs Singlet Energy Transfer in Organic Semiconductors: The Tortoise and the Hare. *J. Phys. Chem. C* **2012**, *116* (33), 17369−17377.
(43) Grisanti, L.; Olivier, Y.; Wang, L. J.; Athanasopoulos, S.; Cornil, J.; Beljonne, D. Roles of Local and Nonlocal Electron-Phonon Couplings in Triplet Exciton Diffusion in the Anthracene Crystal. *Phys. Rev. B: Condens. Matter Mater. Phys.* **2013**, *88* (3), 035450.
(44) Hachmann, J.; Dorando, J. J.; Aviles, M.; Chan, G. K. L. The Radical Character of the Acenes: A Density Matrix Renormalization Group Study. *J. Chem. Phys.* **2007**, *127* (13), 134309.
(45) Kawashima, Y.; Hashimoto, T.; Nakano, H.; Hirao, K. Theoretical Study of the Valence $\pi \rightarrow \pi^*$ Excited States of Polyacenes: Anthracene and Naphthacene. *Theor. Chem. Acc.* **1999**, *102* (1−6), 49−64.
(46) Zeng, T.; Hoffmann, R.; Ananth, N. The Low-Lying Electronic States of Pentacene and Their Roles in Singlet Fission. *J. Am. Chem. Soc.* **2014**, *136* (15), 5755−5764.
(47) Coto, P. B.; Sharifzadeh, S.; Neaton, J. B.; Thoss, M. Low-Lying Electronic Excited States of Pentacene Oligomers: A Comparative Electronic Structure Study in the Context of Singlet Fission. *J. Chem. Theory Comput.* **2015**, *11* (1), 147−156.
(48) White, S. R. Density-Matrix Formulation for Quantum Renormalization-Groups. *Phys. Rev. Lett.* **1992**, *69* (19), 2863−2866.
(49) Chan, G. K. L.; Head-Gordon, M. Highly Correlated Calculations with a Polynomial Cost Algorithm: A Study of the Density Matrix Renormalization Group. *J. Chem. Phys.* **2002**, *116* (11), 4462−4476.
(50) Chan, G. K. L.; Dorando, J. J.; Ghosh, D.; Hachmann, J.; Neuscamman, E.; Wang, H.; Yanai, T. An Introduction to the Density Matrix Renormalization Group Ansatz in Quantum Chemistry. *Prog. Theor. Chem. Phys.* **2008**, *18*, 49−65.
(51) Luo, H. G.; Qin, M. P.; Xiang, T. Optimizing Hartree-Fock Orbitals by the Density-Matrix Renormalization Group. *Phys. Rev. B: Condens. Matter Mater. Phys.* **2010**, *81* (23), 235129.
(52) Sharma, S.; Sivalingam, K.; Neese, F.; Chan, G. K. L. Low-Energy Spectrum of Iron-Sulfur Clusters Directly from Many-Particle Quantum Mechanics. *Nat. Chem.* **2014**, *6* (10), 927−933.
(53) Ottiger, P.; Leutwyler, S.; Koppel, H. Vibrational Quenching of Excitonic Splittings in H-bonded Molecular Dimers: The Electronic Davydov Splittings Cannot Match Experiment. *J. Chem. Phys.* **2012**, *136* (17), 174308.

DOI: 10.1021/acs.jpclett.8b01834
J. Phys. Chem. Lett. 2018, 9, 4087−4095

(54) Scholes, G. D. Long-Range Resonance Energy Transfer in Molecular Systems. *Annu. Rev. Phys. Chem.* **2003**, *54*, 57−87.
(55) Anthony, J. E.; Brooks, J. S.; Eaton, D. L.; Parkin, S. R. Functionalized Pentacene: Improved Electronic Properties from Control of Solid-state Order. *J. Am. Chem. Soc.* **2001**, *123* (38), 9482−9483.
(56) Lee, C. T.; Yang, W. T.; Parr, R. G. Development of the Colle-Salvetti Correlation-Energy Formula into a Functional of the Electron-Density. *Phys. Rev. B: Condens. Matter Mater. Phys.* **1988**, *37* (2), 785−789.
(57) Wadt, W. R.; Hay, P. J. Abinitio Effective Core Potentials for Molecular Calculations - Potentials for Main Group Elements Na to Bi. *J. Chem. Phys.* **1985**, *82* (1), 284−298.
(58) Hollwarth, A.; Bohme, M.; Dapprich, S.; Ehlers, A. W.; Gobbi, A.; Jonas, V.; Kohler, K. F.; Stegmann, R.; Veldkamp, A.; Frenking, G. A Set of D-Polarization Functions for Pseudo-Potential Basis-Sets of the Main-Group Elements Al-Bi and F-Type Polarization Functions for Zn, Cd, Hg. *Chem. Phys. Lett.* **1993**, *208* (3−4), 237−240.
(59) Sun, Q. M.; Berkelbach, T. C.; Blunt, N. S.; Booth, G. H.; Guo, S.; Li, Z. D.; Liu, J. Z.; McClain, J. D.; Sayfutyarova, E. R.; Sharma, S.; Wouters, S.; Chan, G. K. L. PYSCF: The Python-based Simulations of Chemistry Framework. *Wires. Comput. Mol. Sci.* **2018**, *8* (1), e1340.
(60) Sharma, S.; Chan, G. K. L. Spin-adapted Density Matrix Renormalization Group Algorithms for Quantum Chemistry. *J. Chem. Phys.* **2012**, *136* (12), 124121.
(61) Zgid, D.; Nooijen, M. The Density Matrix Renormalization Group Self-Consistent Field Method: Orbital Optimization with the Density Matrix Renormalization Group Method in the Active Space. *J. Chem. Phys.* **2008**, *128* (14), 144116.
(62) Dunning, T. H. Gaussian-Basis Sets for Use in Correlated Molecular Calculations. I. The Atoms Boron through Neon and Hydrogen. *J. Chem. Phys.* **1989**, *90* (2), 1007−1023.
(63) Woon, D. E.; Dunning, T. H. Gaussian-Basis Sets for Use in Correlated Molecular Calculations 0.3. The Atoms Aluminum through Argon. *J. Chem. Phys.* **1993**, *98* (2), 1358−1371.

DOI: 10.1021/acs.jpclett.8b01834
J. Phys. Chem. Lett. 2018, 9, 4087−4095